https://doi.org/10.5194/egusphere-2023-2428
Preprint. Discussion started: 8 November 2023

Source apportionment of particle number size distribution at the street canyon and urban background sites

Sami D. Harni[1*], Minna Aurela[1], Sanna Saarikoski[1], Jarkko Niemi[2], Harri Portin[2], Hanna Manninen[2], Ville Leinonen[3], Pasi Aalto[4], Phil Hopke[5], Tuukka Petäjä[4], Topi Rönkkö[6], Hilkka Timonen[1]

[1] Atmospheric Composition Research, Finnish Meteorological Institute, Helsinki, Finland
[2] Helsinki Region Environmental Services Authority (HSY), Helsinki, Finland
[3] Faculty of Science, Forestry and Technology, Department of Technical Physics, University of Eastern Finland, Finland
[4] Institute for Atmospheric and Earth System Research (INAR) / Physics, Faculty of Science, University of Helsinki, Finland
[5] Department of Public Health Sciences, University of Rochester School of Medicine and Dentistry, Rochester, NY 14642, USA
[6] Aerosol Physics Laboratory, Tampere University, Tampere, Finland

Corresponding author: Sami D. Harni, sami.harni@fmi.fi

Abstract. Particle size is one of the key parameters of aerosol particles affecting their climate and health effects. Therefore, a better understanding of the particle size distributions from different sources is crucial. In urban environments, aerosols are produced in a large number of varying processes, and conditions. This study aims to increase the knowledge of urban aerosol sources using a novel approach to positive matrix factorization (PMF). The particle source profiles are detected in particle number size distribution data measured simultaneously at nearby a street canyon and an urban background station between February 2015 and June 2019 in Helsinki southern Finland. The data is combined into one file so that the data from both stations has the same timestamps. Then PMF finds profiles for the unified data. A total of five different aerosol sources were found. Four of them were detected at both of the stations: slightly aged traffic (TRA2), secondary combustion aerosol (SCA), secondary aerosol (SecA), and long-range transported aerosol (LRT). One of the sources, fresh traffic was only detected at a street canyon. The factors were identified based on available auxiliary data. This work implies that traffic-related aerosols remain important in urban environments and that aerosol sources can be detected by using only particle number size distribution data as input in the positive matrix factorization method.

1 Introduction

Urban aerosol is a complex mixture of particles of different sizes and compositions, originating from multiple anthropogenic and natural sources including, sea salt, fuel combustion (e.g. in thermal power generation, incineration, domestic heating, combustion engines), road, tire, and brake wear, dust, pollen, volcanic ash, forest fires, and industry (Almeida et al., 2006; Guerreiro et al., 2015; Karanasiou et al., 2009). Of these, anthropogenic sources typically dominate urban aerosol concentrations (Guerreiro et al., 2015). The negative health effects related to particulate matter (PM) pollution ($PM_{2.5}$ and

https://doi.org/10.5194/egusphere-2023-2428
Preprint. Discussion started: 8 November 2023

PM_{10}) are commonly accepted and well-documented i.e. (Koenig, 2000; J. Wu et al., 2017) also leading to indirect financial consequences (Johnston et al., 2021). In the recent WHO good practice statement, the systematic measurement of particle number concentration (PNC) of particles ≥ 10 nm is encouraged emphasizing the significance of particle number concentration in addition to PM mass (WHO, 2021).

Source apportionment of aerosols can be done in multiple ways. One often-used method is receptor modeling. Two of the most used receptor modeling methods in aerosol science are principal components analysis (PCA, (Jollife & Cadima, 2016)) and positive matrix factorization (PMF) (Tauler et al., 2009). This work concentrates on PMF which is a mathematical multi-derivative method developed by (Paatero, 1997) and is widely used especially in environmental sciences. PMF can be performed for many different types of data. For example, chemical composition data (e.g. Li et al. 2003; Makkonen et al., 2023), the mass spectra (e.g. (Oduber et al., 2021; Teinilä et al., 2022), particle number size distribution (NSD) (Krecl et al., 2008; Zhou et al., 2005) or a combined matrix with NSD and auxiliary data (Rivas et al., 2020). However, conducting source apportionment solely based on NSD data and using auxiliary data only to verify the sources seems to be challenging and the results are relatively hard to interpret, and/or source profiles might be mixed with multiple sources (Zhou et al., 2005, Jollife & Cadima, 2016, Krecl et al., 2008).

Urban aerosol size distributions have been studied in a comprehensive review of urban aerosols consisting of approximately 200 articles and including 114 cities in 43 countries (T. Wu & Boor, 2021). They stated that in urban environments the majority of particles in terms of number are in the particle size range of 10-100 nm, and the concentrations decrease approximately by a factor of 100 when the particle size increases from 100 nm to 1000 nm. In this study, particle number size distributions were investigated in an urban background and street canyon sites in Helsinki, southern Finland. Earlier studies conducted in the Helsinki metropolitan area have shown that the NSDs vary based on the dominant source. Nucleation-produced particles are the smallest with mode particle sizes of 7-11 nm with traffic-influenced emissions having varying mode particle sizes being 10-75 nm with the smaller particles being produced by nucleation and larger particles being soot mode (Harni et al., 2023; Pirjola et al., 2017; Rivas et al., 2020). Woodburning has been shown to produce slightly larger particles at a mode particle size of 46 nm and to have a wide particle size distribution (Harni et al., 2023; Pirjola et al., 2017). Biogenic emissions have been shown to produce particles with mode sizes between 69-100 nm (Harni et al., 2023; Rivas et al., 2020).

This study aimed to explore how well the sources of urban aerosols are statistically separatable based on the number size distribution data using positive matrix factorization (EPA PMF 5). The factors were identified based on the diurnal cycles of the PMF factors, available supporting data including gases (NO_x, CO_2, O_3), and particle chemistry. The data used in this study was measured in two different sites; Street Canyon (SC) and Urban Background Station (UB) from February 2015 to June 2019. These more than 4-year long datasets also allowed indicative investigation of the trends in NDSs and discussed the reasons for the changes observed in NDSs.

https://doi.org/10.5194/egusphere-2023-2428
Preprint. Discussion started: 8 November 2023

2 Experimental

2.1 Measurement sites

The data used in this study was measured at two different atmospheric measurement stations. The first measurement station is a street canyon (SC) site at Mäkelänkatu in Helsinki Finland (60° 11' 47.53" N, 24° 57' 6.41" E) and it is governed by the Helsinki Region Environmental Services Authority (HSY). The measurement site is situated right beside one of the busiest main roads in Helsinki and is heavily influenced by traffic emissions. The SC measurement site is described in detail by (Barreira et al., 2021). The second station, the urban background (UB) station is located at Kumpula Helsinki SMEAR III (60° 12' 10.41" N, 24° 57' 40.53" E). The site is situated near a park area with a distance of more than 100 m from the nearest busy road. A detailed description of the SMEAR III station is given in (Järvi et al., 2009). The distance between SC and UB stations is approximately 900 m.

2.2 Instruments

Particle number size distribution data used in this work was measured between the 13th of February 2015 and the 5th of June 2019. At the SC site, NSDs were measured with a differential mobility particle sizer (DMPS) consisting of a condensation particle counter (CPC, A 20, Airmodus, Helsinki, Finland) and a Vienna-type differential mobility analyzer (DMA). At the UB site, NSDs were measured with a twin differential mobility particle sizer (Twin-DMPS). The working principle of DMA and response functions are described in detail by Hoppel (1978). The size spectra of DMPS at the SC site were measured in 26-size bins with particle sizes ranging from 6 to 800 nm with a time resolution of approx. 8 min 40 s – 9 min 5 s. The DMPS at the UB-site measured particles in 50-size bins with particle sizes of 3-794 nm with a time resolution of approx 9 min 50 s -10 min 5 s. The charger of the DMPS had difficulties charging the smallest particles on the SC site; therefore, particles smaller than 10 nm were excluded from the analysis for both sites.

Non-refractory PM_1 (organics, sulfate, nitrate, ammonium, chloride) was measured with an aerosol chemical speciation monitor （Q-ACSM, Aerodyne Research Inc., (Ng et al., (2011))) at the SC site. $PM_{2.5}$ and PM_{10} mass concentrations were measured with Tapered Element Oscillating Microbalance (TEOM, model 1405). The Black carbon (BC) concentrations at SC were measured using an Aethalometer (AE33, Magee Scientific). NO_x and O_3 concentrations were measured with Horiba APNA 370 and Horiba APOA-370. At SC CO_2 concentrations were measured with LICOR model LI-7000 and CO with Horiba APMA-360. At UB NO_X and O_3 were measured with TEI42S and TEI49. SO_2 and CO have been measured with Horiba APMA 370 and Horiba, APSA 360.

2.3 Meteorology

Helsinki is a northern city with four different seasons. The total radiance (Itot) and relative humidity (RH) were measured beside the UB at the Helsinki Kumpula weather station (60.203071N, 24.961305E, 24 m asl). The temperature used in this study was measured at Helsinki Kaisaniemi weather station (60.17523N, 24.94459E, 3 m asl, situated 2.4 km south from SC

https://doi.org/10.5194/egusphere-2023-2428
Preprint. Discussion started: 8 November 2023

and 3.2 km from the UB) as the temperature data measured at the Helsinki Kumpula weather had a large gap in late 2017 with missing several months of data. The monthly average relative humidity (RH), temperature (T), and total radiance (I_{tot}) are presented in Fig. 1. The RH reached maximum values during early winter (November-January) and the lowest values were measured during late spring (May). Temperature and radiance on the contrary reached maximum values during the summer months (June-August). The radiance reached the maximum slightly earlier (June-July) than the temperatures (July-August). The highest monthly average temperature was measured during July 2018 (21.3 °C) and the lowest temperature was in January 2016 (-9.2 °C, Fig. 1). In this paper, meteorological data was used in the interpretation of the results.

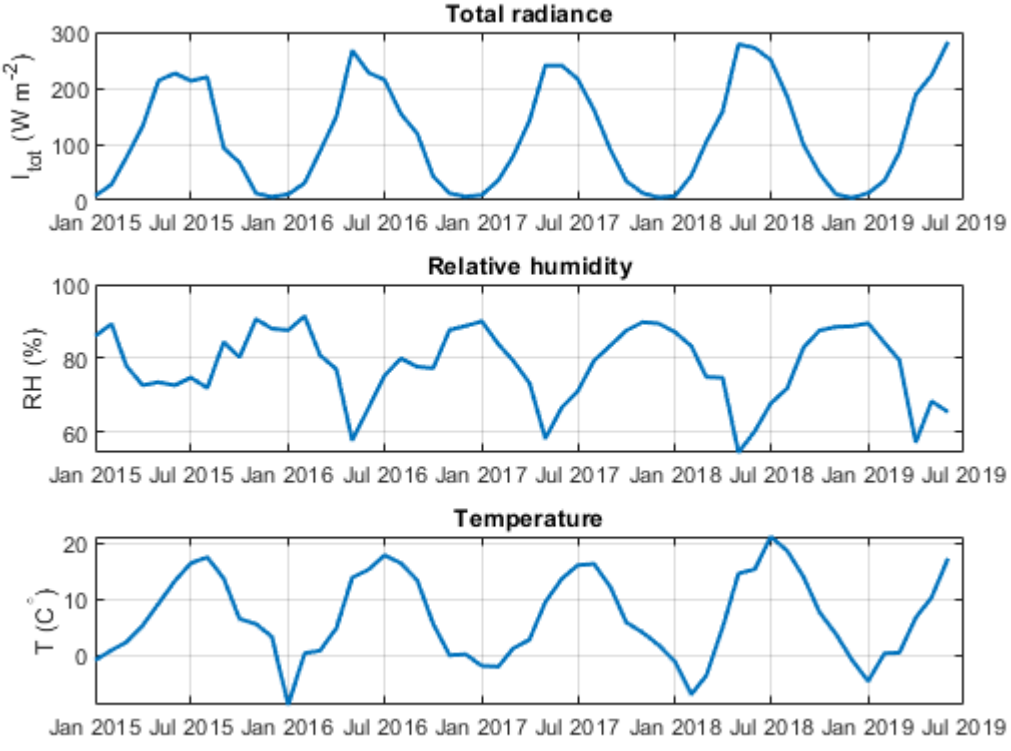

Figure 1: Monthly average values for Total radiance (I_{tot}), Relative humidity (RH), and temperature (T)over the measurement period (2015-2019) at Helsinki.

2.4 Data processing

Strong outliers were removed from the DMPS data by calculating the total concentration and removing the data points that had a concentration ten times larger or smaller than the adjacent measurement points. These relatively relaxed criteria for strong outliers were used as the particle number concentration typically varies significantly in the traffic environment. After removing the outliers, the size distribution data from the DMPS was averaged over one-hour periods to minimize the effect of varying lengths of measurement cycles (approx. 8 min the 40 s – 9 min 5 s at SC and approx 9 min 50 s 10 min 5 s at UB),

https://doi.org/10.5194/egusphere-2023-2428
Preprint. Discussion started: 8 November 2023

and additionally to be able to give matching time stamps to SC and UB data. Only those one-hour data points that had full coverage of data from both stations were included in the subsequent analyses. Averaging is not expected to affect the source profiles significantly and average NSD data has been used in PMF analysis also in previous publications e.g. (Ogulei, Hopke, & Wallace, 2006).

The data analysis was done using a novel method of combing the NSD data from the two measurement stations together so that PMF solved factors for both stations simultaneously. To the knowledge of the authors, this approach has not been used before. Using this approach, the same factors were solved for both sites. So the factor profile which in this case was the size distribution of factor could be slightly different for the stations but the time series would be the same between the stations. If there would be a strong local contribution to some factor then the profile of that factor was significant at one of the stations and near zero at the other. To be able to do this reliably and give even weight to data of both stations the number of bins and the particle size limits needed to be scaled to the same. This was also needed as using too large datafiles was not possible in EPA PMF 5.0. The data was reduced so that both SC and UB NSDs were presented in 16-size bins. So the data matrix consisted of the first 16 columns of SC size bins and the last 16 columns of UB size bins. Data size bins have been modified for positive matrix factorization in other studies. Zhou et al. (2005) for example, reduced 165 bins to 33 by averaging over five bins. In this study, the reduction of bins was done so that a vector with even lognormal bin width was created starting from 1 nm (lognormal width of 0.11 in this study). Then the SC and UB data were interpolated linearly to this diameter vector so that the value for each new diameter point was given as a linear interpolation in a logarithmic x-axis between the nearest original diameters. The new size bin midpoint diameters were: 12.6, 16.2, 20.9, 26.9, 34.7, 44.7, 57.5, 74.1, 95.5, 123, 158, 204, 263, 339, 436.5, and 562 nm. The interpolation needs to be done on a logarithmic x-axis otherwise concentration is overestimated with a negative derivative and underestimated with a positive derivative of the NSD curve. This approach enabled giving the same diameters to both sites regardless of what the original size bins were. This procedure has two drawbacks. One is that the data is leveled slightly as the interpolated values are always between two original values. Therefore the highest peaks are slightly lower and the lowest bottoms are slightly higher than in the original data. The second drawback is that some of the smaller changes in the NSD may be lost. An example of reduced data compared to the original data is presented in Fig. S1.

Source apportionment is typically conducted seasonally (winter, spring, summer, and autumn) among most long-term size distribution source apportionment analyses (Hopke et al., 2022). However, in this study, the data were analyzed in one set to be able to evaluate the changes in the contributions of different factors over the whole measurement period. Rose et al. (2021) have stated that to maintain the representation of the total reliable concentration (N_{tot}) data coverage needs to exceed 50% on the seasonal level and 60 % on the annual level, for the reliable evaluation of diurnal variation a yearly coverage of 75 % was required. The seasonal coverages of the overlapping data for both sites are presented in Table 1. Notable is that the coverages for the first and last seasons (i.e. winter 2015 and summer 2019) were low as the measurement period started and ended in the middle of the seasons.

https://doi.org/10.5194/egusphere-2023-2428
Preprint. Discussion started: 8 November 2023

Table 1: Seasonal overlapping data coverage for urban background (UB) and street canyon (SC) sites.

	Winter (Dec-Feb)	Spring (Mar-May)	Summer (Jun-Aug)	Autumn (Sep-Nov)
2015	14%	81%	92%	92%
2016	62%	70%	88%	90%
2017	86%	49%	89%	91%
2018	73%	48%	84%	93%
2019	85%	88%	5%	-

2.5 Positive Matrix Factorization (PMF)

Positive matrix factorization, developed by (Paatero, 1997), is a multi-derivative method that is widely used in environmental sciences to apportion the sources of the measured data. PMF is a least-squares method that is based on the fact that the matrix X with dimensions n x m can be presented as a product of two matrixes; A with dimensions n x y and B with dimensions of y x m. This can be used so that the matrix n x m is the measured result matrix with n observations and with m species or in the case of NSD particle size bins and y can be set as the number of independent sources.

In estimating error, the methodology was established by (Ogulei, Hopke, Zhou, et al., 2006) and further developed by (Rivas et al., 2020). The measurement uncertainties (σ_{ij}) were calculated with the following equation.

$$\sigma_{ij} = \alpha(N_{ij} + \underline{N}_j)$$

Where α is the arbitrary constant that was chosen similarly as in Rivas et al. (2020) (0.02 for SC and 0.022 for UB) and N_{ij} is the concentration of sample i in size bin column j, and the $\underline{N}_j$ is the arithmetic mean of concentration in size bin j. The overall uncertainty was calculated using the following equation:

$$S_{ij} = \sigma_{ij} + C_3 \cdot N_{ij}$$

Where σ_{ij} is measurement uncertainty, C_3 is an arbitrary constant that was set to 0.1 for UB as in Rivas et al., (2020), but C_3 was set differently at 0.1 while Rivas et al., (2020) had it at 0.18 to better fit the data. N_{ij} is the concentration of bin j of sample i.

Wiedensohler et al. (2012) have stated that the concentration measurement errors seem to be approximately double for particles in the size range 200-800 nm compared to 20-200 nm. Therefore in this study, the measurement errors are corrected for these particle sizes by doubling the α factor.

In this study, the most reasonable solution to fit the data was a five-factor solution based on the testing to produce results with the most meaningful physical interpretation with reasonable residuals. The factors were identified as fresh traffic (TRA1), slightly aged traffic (TRA2), secondary combustion aerosol (SCA), secondary aerosol (SecA), and long-range

https://doi.org/10.5194/egusphere-2023-2428
Preprint. Discussion started: 8 November 2023

transported aerosol (LRT). The dispersion-corrected PMF results were also calculated but the difference to the results calculated without the dispersion correction was found to be negligible. The results calculated with dispersion normalization are presented in supplement Fig. S2. In Fig. 2 the average residual percentages of the measured PN concentrations in different size classes are presented for each size class. The selected solution is seen to explain more than 95 % of the concentration on average with the average residual being always under 10 % for both stations.

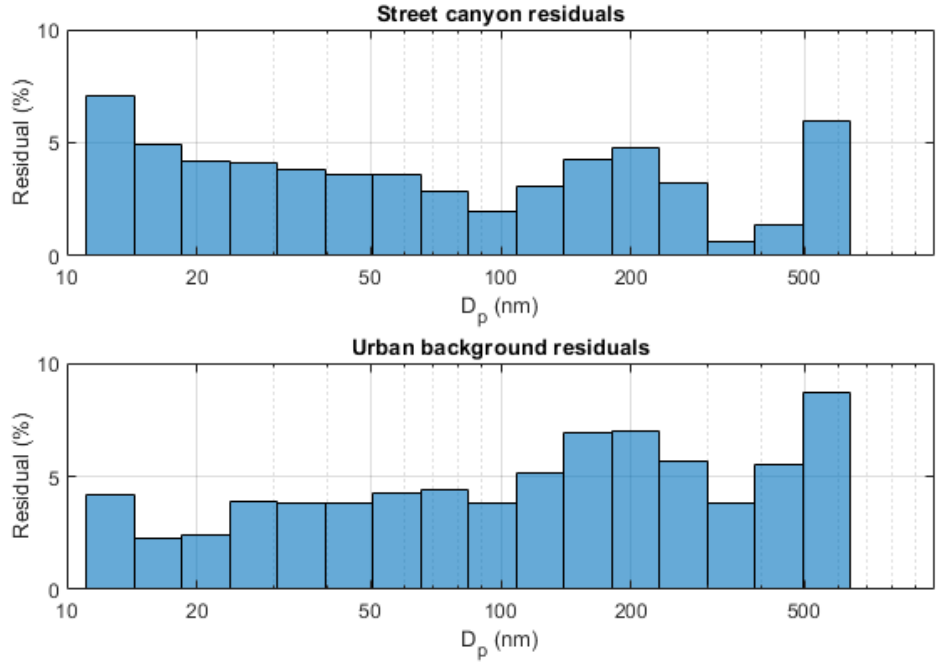

Figure 2: Hourly average residual percentage for each particle size bin for the Street Canyon and Urban background measurement sites.

2.6 Trend analysis

Time series of PMF factors were fitted with trends by using the Theil-Sen estimator developed by Theil (1950) and further developed by Sen (1968). The base level concentrations at the beginning of the measurement period were calculated using the slope determined by the Theil-Sen estimator with each data point and counting the median. Because factors had clear seasonal variance the Then-Seil estimator was plotted in two ways: using the seasonal Thei-Sen estimator where only data from the same months is compared together in forming the estimate. The other way was first removing seasonality from data using the Seasonal-Trend decomposition procedure presented by Cleveland et al. (1990). The seasonal trend removal was needed as the reliability of the results was evaluated using the Mann-Kendall test for monotonic trend (Mann, 1945) which can not be done with seasonal data. The results are presented in Table 3. Figures showing the trend decomposition for the factors and the fitted Theil-Sen estimators are presented in S3-S12. Notably, the trends calculated using the seasonal Theil-

https://doi.org/10.5194/egusphere-2023-2428
Preprint. Discussion started: 8 November 2023

Sen estimator and the Theil-Sen estimator calculated from data without seasonal variability were almost identical increasing the confidence in using seasonal trend decomposition for the data.

3 Results and discussions

3.1 General description of number size distribution

Particle number size distributions were found to be noticeably different for the stations. The time series of the daily average number size distributions in each year are presented in Fig. 3. Figure 3 (lowest panel) presents the R^2 (R-squared) value as a function of particle size when the daily particle number concentrations in each of the 16-size bins are compared between the SC and UB. The observed NSD at SC contained significantly more nanosize particles on many occasions as well as higher overall particle concentrations compared to UB. Notable is that the R^2 value was higher for the larger particle sizes, especially for particles above 200 nm indicating that if the smallest particles are disregarded, the time series would be relatively similar. The higher overall particle number concentration at SC, higher R^2 above 200 nm particles, and lower R^2 below 200 nm particles compared to UB indicate that there was at least one local source producing a lot of nanosize particles at SC that was missing at UB.

https://doi.org/10.5194/egusphere-2023-2428
Preprint. Discussion started: 8 November 2023

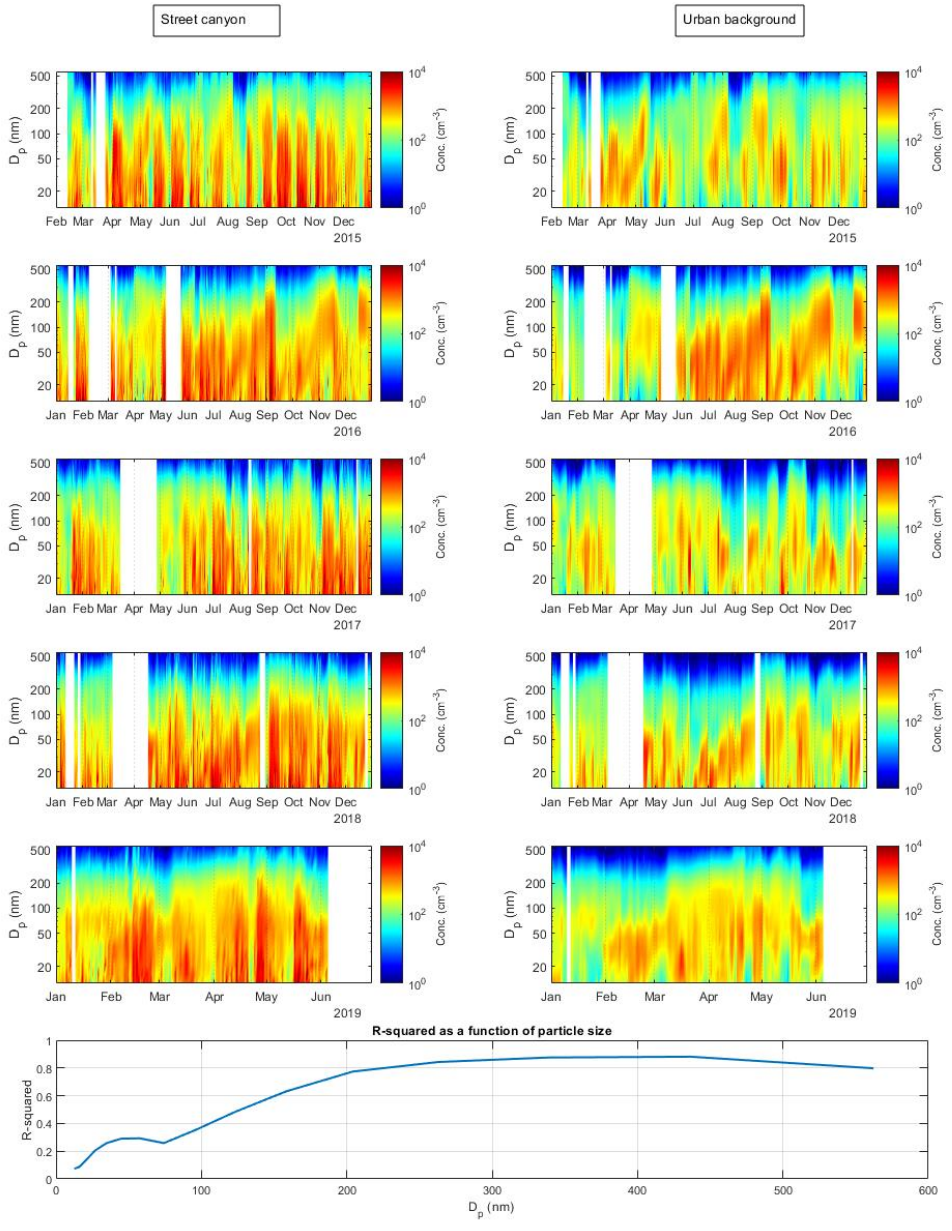

Figure 3: Time series of daily average number size distribution for street canyon (SC) and urban background (UB) for each year (Feb 2015-Jun 2019). The data used is reduced to 16-size bins. In the figure the particle diameter (D_p) is presented on the y-axis, the x-axis presents the time, and particle number concentration (cm^3) has been presented by logarithmic color scale. The correlation between the UB and SC stations (R^2, R-squared) is presented in the bottom plot for the different particle sizes for the daily concentrations.

https://doi.org/10.5194/egusphere-2023-2428
Preprint. Discussion started: 8 November 2023

3.2 Identification of factors

The most reasonable solution in the PMF analysis was a five-factor solution. The factors were identified based on the diurnal profiles, annual variation of the factors, and comparing them to the available auxiliary data measured at the UB and SC sites (trace gases, particle chemistry, PM mass concentrations, and meteorology). The factor profiles and identification variables, their diurnal contributions for workdays and weekends, and monthly contributions are presented in Fig. 4 and Table 2. The contributions presented in Fig. 4 are the coefficients with which to multiply the factor profile at each time to get the real contribution.

Table 2: PMF factors, their size modes, correlating variables, and identification.

Factor	PN size mode (nm)	Important correlating variables	Identification arguments
TRA1 – fresh traffic emissions from the immediate vicinity of the site	12.6	BC, NO, NO_2, and NO_x at SC	Particle size, and diurnal similar to traffic intensity. Correlation with traffic tracers.
TRA2 – slightly aged (minutes to an hour) traffic emissions	16.2	NO_x and NO at UB	Diurnal is similar to traffic. Slightly behind TRA1
SCA – Secondary combustion aerosol	44.7	NO_x at UB, mz60	Delayed peak after TRA1 and TRA2 correlation with NO_x at UB
SecA – secondary aerosol	74.1	Total organics, mz43	No difference between workdays and weekends, highest concentrations in summer.
LRT – long-range transported aerosol	204	$PM_{2.5}$, SO_4, NO_3 and total organics	Correlations with variables related to LRT and minimal diurnal profile

https://doi.org/10.5194/egusphere-2023-2428
Preprint. Discussion started: 8 November 2023

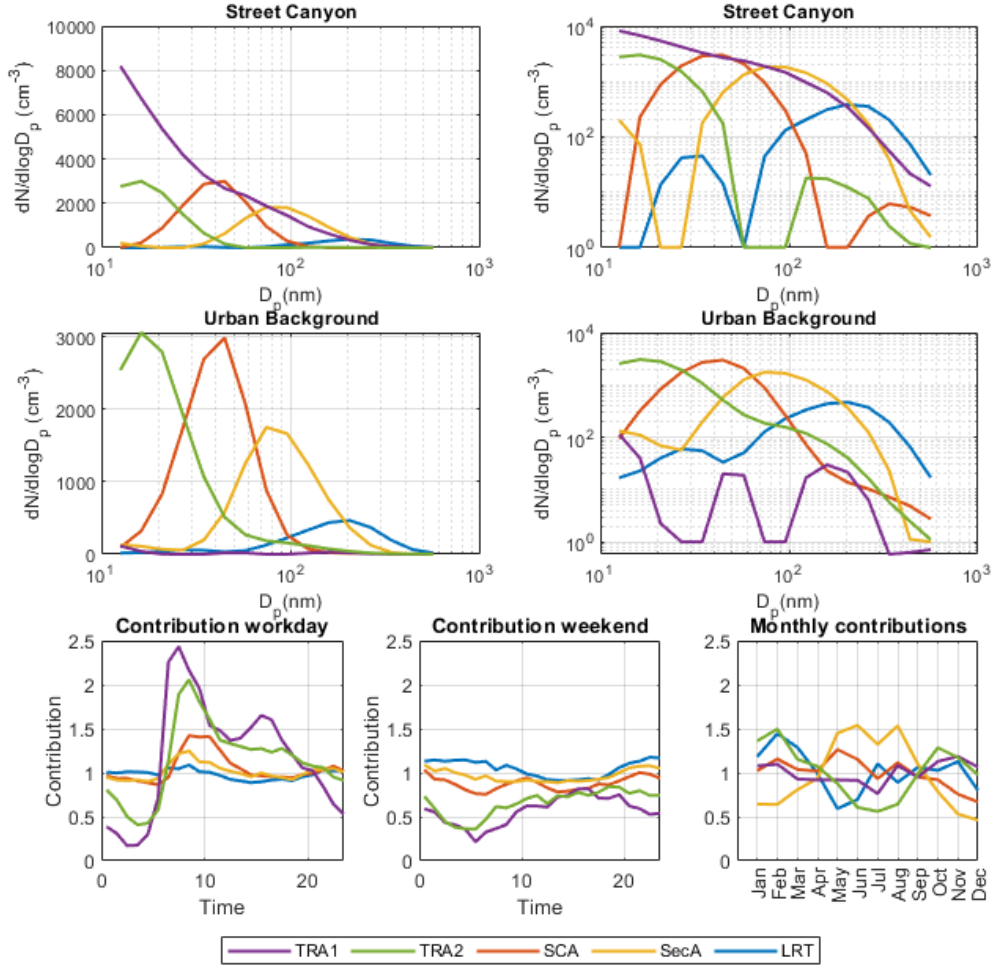

Figure 4: Positive matrix factorization (PMF) factors presented in linear and logarithmic y-axes for Street Canyon (upper plot) and Urban background (middle plot) sites and their hourly relative contributions (lower plot) during workdays, weekends, and months. Note that the linear scale for the plots is different. The value presented in contribution figures is the factor with which to multiply the factor profile at any current time to get the total contribution. The average for the contribution factor is 1 over the whole measurement period for all the factors.

TRA1 was interpreted to represent particles that originate from the local traffic emissions in the immediate proximity of the measurement station. This factor was the dominant factor in SC while it was almost zero at UB, which was located on a hill over 100 m from the nearest busy road. TRA1 had the highest number of particles in the smallest measured particle size (12.6 nm) and the second mode at around 50-60 nm. Possibly, a third mode at 100-200 nm can be seen as a tail in the log-log plot (Fig. 4). Similar nonvolatile modes at 10 nm and 70 nm particle diameters have been reported for laboratory measurements for modern gasoline cars (Karjalainen et al., 2014). Also, Rönkkö et al., (2017) have shown that traffic produces significant concentrations of nanocluster aerosol in urban traffic environments. During weekdays TRA1 had a distinctive diurnal profile, similar to BC and NO_x, which are often related to traffic emissions with the largest peak during

https://doi.org/10.5194/egusphere-2023-2428
Preprint. Discussion started: 8 November 2023

the morning rush hour and the second, slightly lower peak during the afternoon rush hour (Fig. 5). TRA1 had significantly lower contributions during weekends, but a high correlation withNO_x and BC. Overall, the Pearson correlation coefficients (R) for TRA1 with BC (AE33 with 880 nm) and NO_x were 0.76 and 0.85 at SC, respectively. TRA1 had also a high correlation with NO_2 and NO at SC (Table 3).

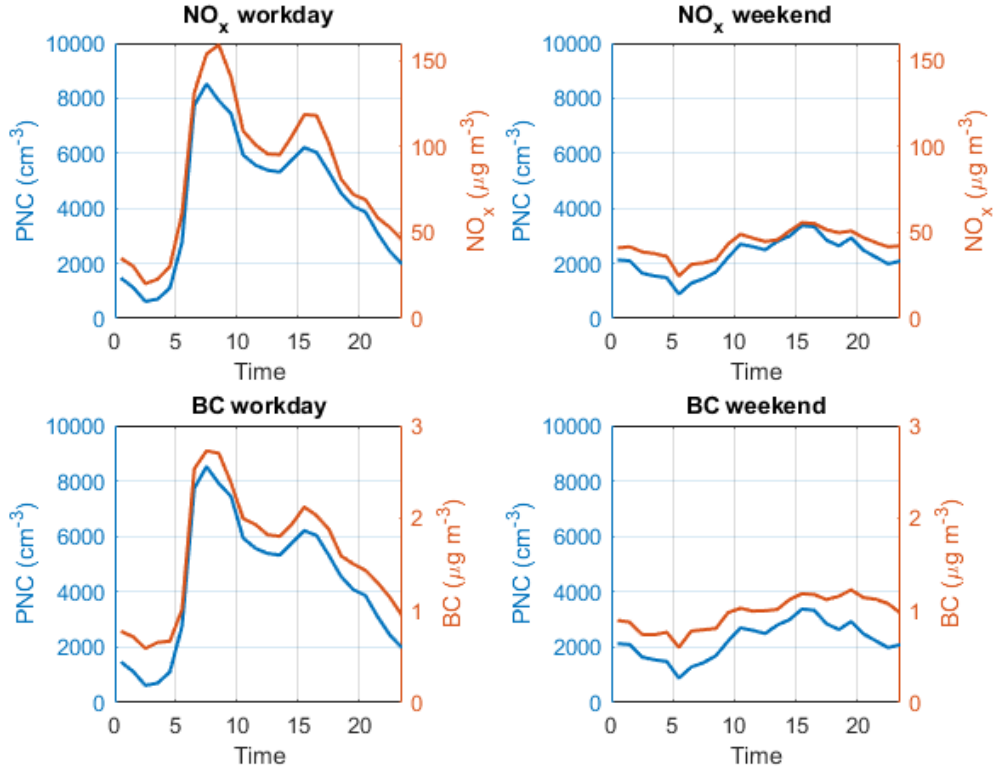

Figure 5: Average hourly TRA1 factor-related particle number concentrations at the street canyon marked with blue presented with NO_x and BC_{880} at the street canyon measurement site for workdays and weekends. 2015-2019.

TRA2 factor was interpreted as a slightly aged (~minutes to an hour), atmospherically processed (e.g., cooling, dispersion, mixing), traffic-related factor. It had a maximum mode particle size of 16.2 nm at both stations. The mode particle size was larger than for TRA1 which was logical as during dilution and cooling, the precursor gases condense on primary particles growing the particle size (Ning & Sioutas, 2010). TRA2 also had a diurnal trend that matches the traffic pattern having a peak during the morning rush hour and elevated concentrations for the rest of the working hours of the day (Fig. 4). The morning peak was noticed approximately 1 h later compared to the TRA1 factor. Therefore the TRA2 can be considered slightly aged traffic emissions, originating from a slightly larger area. The most significant correlations of TRA2 with auxiliary data were with NO_x and NO measured at UB. (Table 1). This also supports the slightly aged character of TRA2 as the SC site was dominated by immediate traffic-caused emissions (Fig. 4). The TRA2 had higher concentrations during

https://doi.org/10.5194/egusphere-2023-2428
Preprint. Discussion started: 8 November 2023

colder moths which might be because in cold temperatures VOCs condense more efficiently on existing particles (Fig. 4). In addition, the boundary layer is shallower during cold months enhancing the accumulation of pollutants.

The secondary combustion aerosol (SCA) factor had a peak particle size of 44.7 nm at both sites and was interpreted as a secondary aerosol originating from combustion processes i.e. liquid fuel (e.g., gas, diesel, oil) or solid fuel (e.g., biomass, coal) combustion. SCA was seen to have relatively weak correlations with the auxiliary data as could be expected for atmospherically processed aerosol. The strongest Pearson correlation coefficient of 0.56 was found with NO_x at the UB site (Table 3) both having very similar diurnals during both workdays and weekends (Fig. 6). The highest peak of the SCA was seen approximately 3 hours later compared to the TRA1 factor indicating that the factor included traffic emissions that have been aged/processed a couple of hours in the atmosphere. SCA factor was found to have an evening peak in addition to the morning rush hour peak. The evening peak was more pronounced during weekends which indicates there might be contributions from biomass combustion. In an earlier study, BC originating from biomass combustion has been shown to contribute 15 ± 14 % at SC and between 41 ± 14 and 46 ± 15% of the BC in residential-detached house areas (Helin et al., 2018). To support this the diurnal trends of SCA and organic fragment at m/z 60 (Q-ACSM) at SC were plotted (Fig. 6). The fragment at m/z 60 and especially its fraction of total OA have widely been used as a marker for primary wood combustion emissions (Alfarra et al., 2007). The m/z 60 was seen to correlate well with the evening peak at SC strengthening the assumption of wood combustion contribution. Interestingly, m/z 60 was elevated also during the morning rush hour suggesting also a traffic-related source for this ion. The similar diurnal profiles of m/z60 only act as indications of biomass combustion contributions.

https://doi.org/10.5194/egusphere-2023-2428
Preprint. Discussion started: 8 November 2023

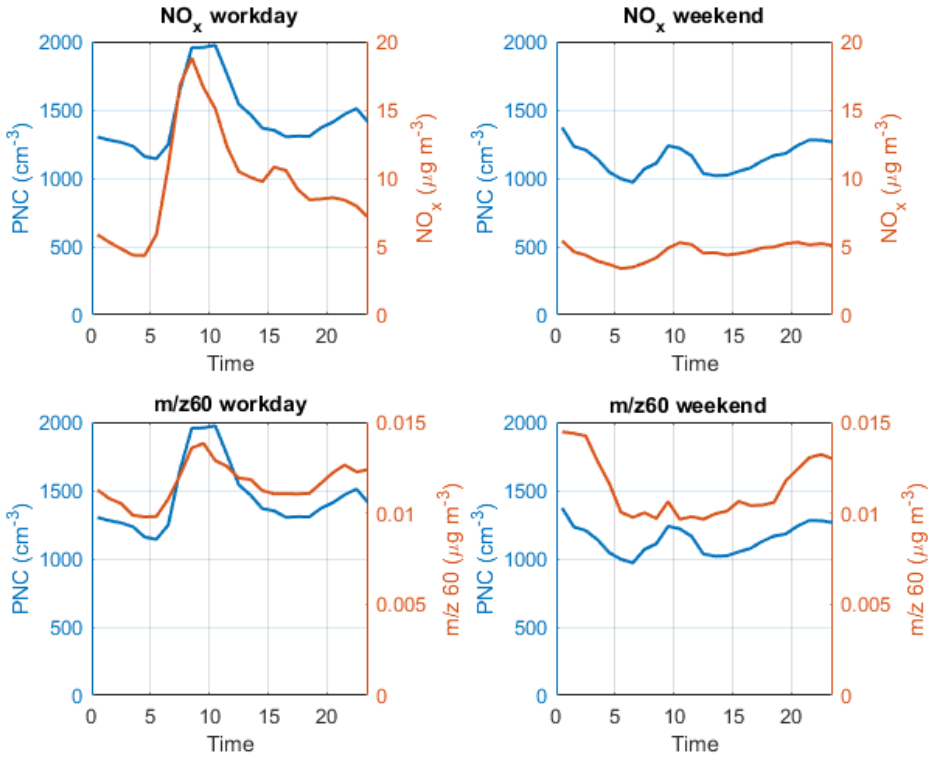

Figure 6: Diurnal trends for SCA factor-related concentrations at SC and, NO_x concentration at Urban background station and organic fragment at m/z60 concentrations at SC and their diurnal profiles during workdays and weekends.

The secondary aerosol (SecA) factor had a peak particle size of 74.1 nm in both sites and was interpreted as an aged, photochemically formed secondary aerosol from biogenic and anthropogenic precursors. This assumption is based on the negligible difference in diurnal profiles between workdays and weekends and elevated contribution during the summer months with the highest total radiance (Fig. 1 and 4.). Additionally, the strongest correlations of the SecA factor were with total organics and m/z 43. (Table 3). Anthropogenic and biogenic VOCs are shown to be important SecA precursors in a traffic environment (Saarikoski et al., 2023). However, the SecA factor also somewhat correlates with BC (Table 3) possibly indicating that BC particles that are ubiquitous in traffic environments might act as cores for SecA particles.

The long-range transport factor (LRT) had a peak particle size at 204 nm in both sites and is interpreted as a long-range transport as it had strong correlations with $PM_{2.5}$, SO_4, NO_3, and organics (Table 3). The correlation was even higher (0.80) with the sum of NO_3 and SO_4 at the SC. Typically higher concentrations of accumulation mode particles have been observed during the LRT events (Timonen et al., 2008). Furthermore, Niemi et al. (2009) have shown relatively high concentrations of inorganic ions, especially SO_4 NH_4, and BC are typically observed during the LRT events. The correlation of LRT with NH_4 was relatively high but the correlation with BC was quite low (Table 3). The reason for the low correlation with BC might be due to local sources of BC e.g. traffic and the short atmospheric lifetime of BC (Cape et al., 2012). Also, Niemi et al. (2009)

https://doi.org/10.5194/egusphere-2023-2428
Preprint. Discussion started: 8 November 2023

did not report high concentrations of NO_3 during the LRT episodes, likely because of evaporation losses of ammonium
280 nitrate from the filters. However, more recent studies with online analysis of NO_3 have linked elevated NO_3 concentrations to LRT episodes in the area (Harni et al., 2023; Barreira et al., 2021; Pirjola et al., 2017). Also, elevated PM_1 and $PM_{2.5}$ concentrations have been related to the LRT episodes in the area. (Harni et al., 2023; Barreiraet al., 2021; Niemi et al., 2009; Pirjola et al., 2017)

285 **Table 3: Pearson correlation coefficients of the PMF solution factors (LRT, SCA, SecA TRA1, and TRA2) with other factors and other measured parameters (with NO_x, O_3, SO_2, NO, CO from UB station and NO, NO_x, NO_2, PM_{10}, $PM_{2.5}$ PM_{coarse}, O_3, CO, BC_{880}(AE33), CO_2, PM_{tot}, ORG_{43}, ORG_{57}, ORG_{60}Chl, NH_4, NO_3, ORG_{tot} and SO_4 from SC, Total radiation (I_{tot}), and RH from Kumpula wether station and Temperature (T) from Kaisaniemi weather station.**

	LRT	SCA	SecA	TRA1	TRA2
NO_x (UB)	0.19	0.56	0.46	0.33	0.48
O_3 (UB)	-0.19	-0.25	-0.08	-0.24	-0.32
SO_2 (UB)	0.05	0.21	0.09	0.04	0.13
NO (UB)	0.12	0.44	0.34	0.2	0.42
CO (UB)	0.33	0.32	0.23	0.17	0.34
NO (SC)	0.05	0.36	0.27	0.82	0.32
NO_x (SC)	0.06	0.38	0.31	0.85	0.33
NO_2 (SC)	0.08	0.39	0.36	0.8	0.3
PM_{10} (SC)	0.12	0.23	0.23	0.42	0.2
$PM_{2.5}$ (SC)	0.74	0.24	0.45	0.36	0.11
PM coarse (SC)	-0.07	0.11	0.06	0.22	0.13
O_3 (SC)	-0.09	-0.2	-0.07	-0.39	-0.28
CO (SC)	-0.06	-0.02	-0.11	-0	0.14
BC_{880} (SC)	0.26	0.35	0.44	0.76	0.24
CO_2 (SC)	0.03	0.02	0.1	0.11	-0.04
PM_{tot} (SC)	0.09	0.26	0.31	0.46	0.16
ORG_{43}	0.54	0.18	0.63	0.23	-0.03
ORG_{57} (SC)	0.35	0.36	0.52	0.59	0.16
ORG_{60} (SC)	0.64	0.24	0.5	0.21	0.07
Chl (SC)	0.25	0.04	0.07	0.02	0.03
NH_4 (SC)	0.62	0.04	0.12	0.07	-0.01
NO_3 (SC)	0.69	0.16	0.22	0.15	0.03
ORG_{tot} (SC)	0.64	0.2	0.65	0.25	-0.03
SO_4 (SC)	0.71	0.01	0.11	-0.03	-0.05
I_tot	-0.12	0.05	0.16	0.05	-0.02
RH	0.24	-0.05	-0.09	0.07	-0.06
T	-0.03	-0.06	0.32	-0.03	-0.3
LRT	1	0.01	0.26	-0	-0.04
SEC	0.01	1	0.37	0.21	0.3
SOA	0.26	0.37	1	0.13	0.02
TRA1	-0	0.21	0.13	1	0.23
TRA2	-0.04	0.3	0.02	0.23	1

https://doi.org/10.5194/egusphere-2023-2428
Preprint. Discussion started: 8 November 2023

3.3 Monthly average contributions and trends of factors

Figure 7 represents the time series for the contributions of the PMF factors to PNC at the SC and urban UB sites. The average monthly contributions at the SC site were 52, 15, 17, 13, and 3 % for TRA1, TRA2, SCA, SecA, and LRT, respectively. For the UB the corresponding monthly average contributions were 1, 36, 34, 23, and 7 % for TRA1, TRA2, SCA, SecA, and LRT, respectively. TRA1 factor was seen to be the main contributor to PNC at SC while at UB the PNC was usually dominated by the slightly aged combustion-related factors, TRA2 and SCA, with quite similar contributions, as could be expected for stations situated next to the road and 100 m away from the road. During summertime also SecA had a contribution that was roughly even with TRA2 and SCA in both stations, highlighting the importance of secondary aerosol formation even in urban environments. Similar contributions of traffic-related aerosols either fresh (46%) like TRA1 in this study or aged (27 %) like TRA2+SCA (sum 28 %) have been reported in the roadside environment (Al-Dabbous & Kumar, 2015).

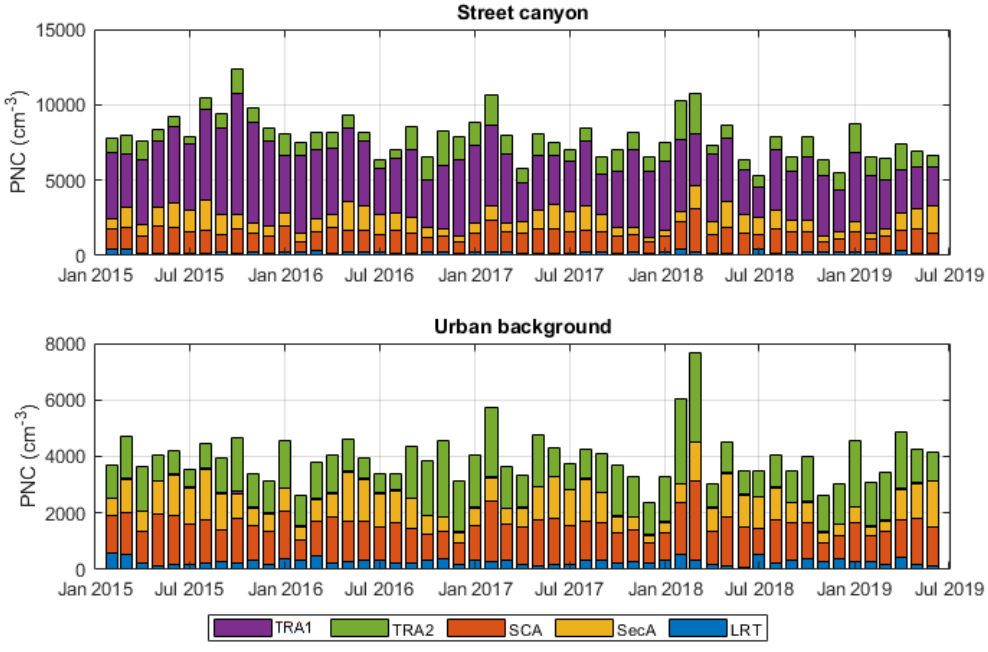

Figure 7: Contribution of different factors to particle number concentrations (PNC) at the street canyon and urban background site.

The contributions of factors in SC and UB stations were also calculated in terms of particle volume. Notably, the contributions of factors were very different when the particle volume was considered (Fig. 8). The average monthly contributions were 28, 1, 4, 26, and 41 % TRA1, TRA2, SCA, SecA, and LRT, respectively, for SC. For UB the monthly average contributions were 1, 5, 7, 29, and 59 % for TRA1, TRA2, SCA, SecA, and LRT, respectively. Compared to PNC, the contributions of TRA1, TRA2, and SCA decreased whereas those of SecA and especially LRT increased. The largest

https://doi.org/10.5194/egusphere-2023-2428
Preprint. Discussion started: 8 November 2023

contributor to volume concentration was LRT followed by SecA at UB. At SC the second largest contributor to particle volume during summer months was also the SecA but during winter the second largest contributor was TRA1.

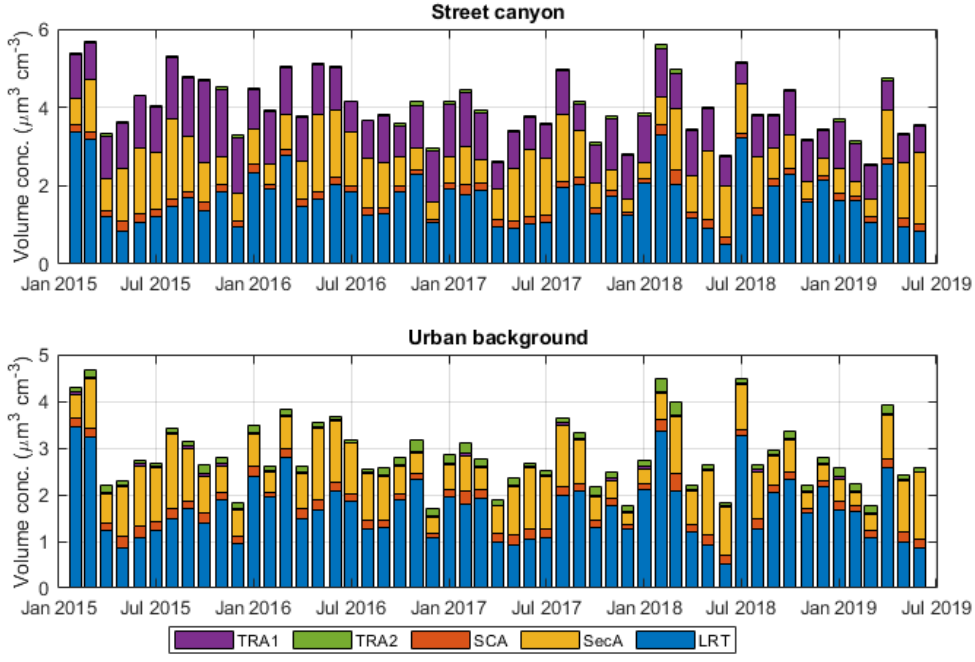

Figure 8: Monthly average volume-based contributions of different factors at the SC and UB stations during the measurement period.

Regarding the trends in the factor concentrations, three trends with statistical significance were found: decreasing trends of -9.5 and -6.5 % yearly for TRA1 and SecA respectively, and an increasing trend of 6.4 yearly for TRA2 (Table 4). The decreasing trend of TRA1 seems to imply that the primary emissions from traffic have been reducing over the years. This is supported by the fact that the vehicle fleet has renewed rapidly in Finland between the years 2015 and 2019. For instance, the proportions of low-emission (EURO 6/VI grade) vehicles in driven kilometers have increased in different vehicle classes in Finland as follows; cars from 6% to 29%, vans from 1% to 25%, and trucks from 7% to 31% (VTT's LIPASTO calculation system for traffic exhaust emission in Finland). The proportion of low-emission city buses has increased particularly quickly in the Helsinki metropolitan area, from 17% to 59% during the 5 years (statistics from the Helsinki Regional Transport Authority HSL). The impact of bus emissions is significant at the Mäkelänkatu site since there is a bus lane very close (0.5 m) to the air quality monitoring station. Notable is still that the slightly aged traffic-related emissions (TRA2) have increased. That can be speculated to be due to the change in the engine and after-treatment techniques of the vehicles and emphasizes the significance of atmospheric processes on traffic emissions

The decrease of the SecA factor is difficult to explain as it was speculated to have both anthropogenic and biogenic sources. The latter is closely connected to biogenic sources and meteorology (temperature and light) and the former to the

https://doi.org/10.5194/egusphere-2023-2428
Preprint. Discussion started: 8 November 2023

development of technology. In the previous chapter, SecA concentrations were shown to somewhat correlate with BC, which was suggested to be due to the BC particles acting as cores for SecA. In fact, the decreasing trend was similar to earlier presented BC trends (decrease between -10 and -6% yr^{-1}) in different environments (traffic, urban background, and regional background) in Finland (Luoma et al., 2021). More data (years) are needed to see if the decreasing trend was real as the larger the sample size is, the better the hypothetical test is. Table 4 presents all the results of the trend analysis.

Table 4: Seasonal Theil-Sen estimators and Theil-Sen estimators calculated from data with seasonality removed with confidence levels and base level concentrations at the beginning of the measurement period for TRA1, TRA2, SCA, SecA, and LRT.

		TRA1	TRA2	SCA	SecA	LRT
Seasonal Then-Seil estimator	Base concentration (cm^{-1})	5175	953	1445	1073	214
	Yearly change (cm^{-1})	-493	61	-32	-70	-6
	Relative change (%)	-9.5	6.4	-2.2	-6.5	-2.7
Theil-Sen estimator for data with no seasonality	Base concentration (cm^{-1})	5149	953	1407	1074	210
	Yearly change (cm^{-1})	-471	62	-11	-70	-5
	Relative change (%)	-9.1	6.5	-1	-6.6	-2.3
	Significance	yes	yes	no	yes	no

Conclusions and summary

Particle size is one of the most important parameters of atmospheric particles since it impacts the climate and health effects of particles. In this study, the origin and characteristics of particle number size distribution were investigated in Helsinki, southern Finland. The measurements were carried out at two sites an urban background and a street canyon site, between 2015 and 2019. The source apportionment based solely on the particle number size distribution data was performed using

https://doi.org/10.5194/egusphere-2023-2428
Preprint. Discussion started: 8 November 2023

positive matrix factorization. A novel approach to analyze the data was used as the particle number size distribution data were combined from two different nearby sites. As a result, the same factors with the same time series were obtained for both sites, only with different profiles. If a similar profile was seen at both sites the source was considered regional.

In total, 5 factors were found in the data: fresh traffic (TRA1), slightly aged traffic (TRA2), secondary combustion aerosol (SCA), secondary aerosol (SecA), and long-range transported aerosol (LRT). Three of the factors were related to traffic. TRA1 had a clear diurnal profile with the largest peak during the morning rush hour and the second, slightly lower peak during the afternoon rush hour. TRA2 peaked approximately 1 h later compared to the TRA1 factor indicating slight processing in the atmosphere while SCA had a maximum of three hours later than TRA1 being much more aged. SCA had an evening peak in addition to the morning rush hour peak, which indicated that it might have originated from both liquid fuel (mainly traffic) and solid fuel (biomass) combustion. TRA1 factor was the main contributor to PNC at SC while at UB the PNC was usually dominated by the slightly aged combustion-related factors, TRA2 and SCA. During summertime also SecA had a significant contribution to aerosol particle number concentrations at both stations.

The trend analysis revealed that TRA1 and SecA have been decreasing by 9.1 and 6.6 % yearly. For TRA2, an increasing trend of 6.5 % yearly was discovered. These findings indicate that the properties of particle emissions originating from traffic have changed in recent years, probably due to the changes in the vehicle engine and after-treatment techniques. The significant decreasing trend for TRA1 implies that while the improving emission reduction techniques seem to be reducing immediate emissions of traffic, the slightly aged traffic emissions are even increasing as an increasing trend was observed for TRA2. This change in vehicle fleet is not only related to the direct emission as the decrease of SecA can be speculated to be linked to the decrease of core particle concentrations, such as BC.

The SCA factor seemed to be a mix of aged traffic particles and particles from biomass combustion. Although the contribution from biomass combustion in traffic environment includes high uncertainty. Also, all the factors had more than one mode. Therefore, in addition to the particle size bins, adding the auxiliary data to the PMF analysis might improve the separation between the different factors. However, the novel method of attaching simultaneous data from two different sites seems to improve the detection of different factors and could be useful in locations where there is NSD data available from more than one site.

In conclusion, traffic remains a large contributor to ambient particle number concentrations in urban environments despite the decreasing trend caused by the improvements in emission reduction technologies and electrification of the traffic fleet. Additionally, while the primary emissions have reduced the effect on the secondary aerosols is more uncertain as in this study the concentrations of slightly aged aerosols were increasing. Therefore studying how the emissions age in the atmosphere is important in the future. Additionally, the study demonstrated that detecting aerosol source factors purely based on NSD data is possible, but attaching the factors to individual sources would be difficult without available auxiliary data.

https://doi.org/10.5194/egusphere-2023-2428
Preprint. Discussion started: 8 November 2023

Data availability

Data is available upon request from the corresponding author Sami Harni (sami.harni@fmi.fi)

Supplement

Author contributions

SDH made the formal analysis, software, and visualization and wrote the original draft of the paper. MA, SS, and JN contributed to the conceptualization and writing by reviewing and editing the article. HP, PA, and HM contributed to the investigation. VL contributed to the formal analysis reviewing and editing of the article. PH contributed to the formal analysis. TP and TR contributed to editing and rewriting the article. HT acted as a supervisor and contributed to the conceptualization reviewing and editing of the article.

Competing interests

One of the co-authors is a member of the editorial board of Atmospheric Chemistry and Physics.

Acknowledgments

This work was supported by the European Union's Horizon Europe research and innovation programme under grant agreement No 101096133 (PAREMPI: Particle emission prevention and impact: from real-world emissions of traffic to secondary PM of urban air), from European Union Horizon 2020 research and innovation programme under grant agreement No (TUBE), from European Union Horizon 2020 research and innovation programme under Grant agreement No 101036245 (RI-URBANS). Financial support from Urban Air Quality 2.0 project funded by Technology Industries of Finland Centennial Foundation and from Black Carbon Footprint project funded by Business Finland (Grant 528/31/2019) and participating companies is acknowledged.

References

Al-Dabbous, A. N., & Kumar, P.: Source apportionment of airborne nanoparticles in a Middle Eastern city using positive matrix factorization, Environ. Sci. Proces. & Impacts, 17(4), 802–812. https://doi.org/10.1039/C5EM00027K, 2015.

Alfarra, M. R., Prevot, A. S. H., Szidat, S., Sandradewi, J., Weimer, S., Lanz, V. A., Schreiber, D., Mohr, M., & Baltensperger, U.: Identification of the mass spectral signature of organic aerosols from wood burning emissions, Environ. Sci. Technol., 41(16), 5770–5777. https://doi.org/10.1021/es062289b, 2007.

https://doi.org/10.5194/egusphere-2023-2428
Preprint. Discussion started: 8 November 2023

Almeida, S. M., Pio, C. A., Freitas, M. C., Reis, M. A., & Trancoso, M. A.: Source apportionment of atmospheric urban aerosol based on weekdays/weekend variability: Evaluation of road re-suspended dust contribution. Atmos. Environ., 40(11), 2058–2067. https://doi.org/10.1016/j.atmosenv.2005.11.046, 2006.

Barreira, L., Helin, A., Aurela, M., Teinila, K., Friman, M., Kangas, L., v. Niemi, J., Portin, H., Kousa, A., Pirjola, L., Ronkko, T., Saarikoski, S., & Timonen, H.: In-depth characterization of submicron particulate matter inter-annual variations at a street canyon site in northern Europe. Atmos. Chem. Phys., 21(8), 6297–6314. https://doi.org/10.5194/acp-21-6297-2021, 2021.

Cape, J. N., Coyle, M., & Dumitrean, P.: The atmospheric lifetime of black carbon. Atmos. Environ., 59, 256–263. https://doi.org/10.1016/J.ATMOSENV.2012.05.030, 2012.

Cleveland, R. B., Cleveland, W. S., & Terpenning, I.: STL: A seasonal-trend decomposition procedure based on loess. J. Off. Stat., 6(1), 3., 1990.

Guerreiro, C., de Leeuw, F., & Ortiz, E. E. A. A. G.: Air quality in Europe — 2015 report. In Report (Issue 5). papers2://publication/uuid/1D25F41B-C673-4FDA-AB71-CC5A2AD97FDD, 2015.

Harni, S. D., Saarikoski, S., Kuula, J., Helin, A., Aurela, M., Niemi, J. V., Kousa, A., Rönkkö, T., & Timonen, H.: Effects of emission sources on the particle number size distribution of ambient air in the residential area. Atmos. Environ., 293(October 2022). https://doi.org/10.1016/j.atmosenv.2022.119419, 2023.

Helin, A., Niemi, J. v., Virkkula, A., Pirjola, L., Teinilä, K., Backman, J., Aurela, M., Saarikoski, S., Rönkkö, T., Asmi, E., & Timonen, H.: Characteristics and source apportionment of black carbon in the Helsinki metropolitan area, Finland. Atmos. Environ., 190(July), 87–98. https://doi.org/10.1016/j.atmosenv.2018.07.022, 2018.

Hering, S. v., Kreisberg, N. M., Stolzenburg, M. R., & Lewis, G. S.: Comparison of Particle Size Distributions at Urban and Agricultural Sites in California's San Joaquin Valley. Aerosol Sci. Technol., 41(1), 86–96. https://doi.org/10.1080/02786820601113290, 2007.

Hopke, P. K., Feng, Y., & Dai, Q.: Source apportionment of particle number concentrations: A global review. Sci. Total Environ., 819, 153104. https://doi.org/10.1016/j.scitotenv.2022.153104, 2022.

Hoppel, W.: Determination of the aerosol size distribution from the mobility distribution of the charged fraction of aerosols. J. Aerosol Sci., 9(1), 41-54. https://doi.org/10.1016/0021-8502(78)90062-9, 1977.

Järvi, L., Hannuniemi, H., Hussein, T., Junninen, H., Aalto, P. P., Hillamo, R., Mäkelä, T., Keronen, P., Siivola, E., Vesala, T., & Kulmala, M.: The urban measurement station SMEAR II: Continuous monitoring of air pollution and surface-atmosphere interactions in Helsinki, Finland. Boreal Environ. Res., 14(SUPPL. A), 86–109., (2009).

Johnston, F. H., Borchers-Arriagada, N., Morgan, G. G., Jalaludin, B., Palmer, A. J., Williamson, G. J., & Bowman, D. M. J. S.: Unprecedented health costs of smoke-related PM2.5 from the 2019–20 Australian megafires. Nat. Sustain., 4(1), 42–47. https://doi.org/10.1038/s41893-020-00610-5, 2021.

Jollife, I. T., & Cadima, J.: Principal component analysis: A review and recent developments. Philos. Trans. Royal Soc. A, 374(2065). https://doi.org/10.1098/rsta.2015.0202, 2016.

Karanasiou, A. A., Siskos, P. A., & Eleftheriadis, K.: Assessment of source apportionment by Positive Matrix Factorization analysis on fine and coarse urban aerosol size fractions. Atmos. Environ., (Vol. 43, Issue 21, pp. 3385–3395). https://doi.org/10.1016/j.atmosenv.2009.03.051, 2009.

Karjalainen, P., Pirjola, L., Heikkilä, J., Lähde, T., Tzamkiozis, T., Ntziachristos, L., Keskinen, J., & Rönkkö, T.: Exhaust particles of modern gasoline vehicles: A laboratory and an on-road study. Atmos. Environ., 97, 262–270. https://doi.org/10.1016/j.atmosenv.2014.08.025, 2014.

Koenig, J. Q.: Health Effects of Particulate Matter. Health Effects of Ambient Air Pollution, 115–137. https://doi.org/10.1007/978-1-4615-4569-9_10, 2000.

Krecl, P., Hedberg Larsson, E., Ström, J., & Johansson, C.: Contribution of residential wood combustion and other sources to hourly winter aerosol in Northern Sweden determined by positive matrix factorization. Atmos. Chem. Phys., 8(13), 3639–3653. https://doi.org/10.5194/acp-8-3639-2008, 2008.

Li, A., Jang, J.-K., Scheff, P.A.: Application of EPA CMB8.2 model for source apportionment of sediment PAHs in Lake Calumet, Chicago. Environ. Sci. Technol. 37, 2958–2965.0. https://doi.org/10.1021/es026309v, 2003.

Makkonen, U., Vestenius, M., Huy, L.N., Anh, N.T.N., Linh, P.T.V., Thuy, P.T., Phuong, H.T.M., Nguye, H., Thuy, L.T., Aurela, M., Hellén, H., Love, K., Kouznetsov, R., Kyllönen, K., Teinilä, K., Oanh, N.T.K. Chemical composition and potential sources of $PM_{2.5}$, in Hanoi. Atmos. Env., 299(2023), 119650. https://doi.org/10.1016/j.atmosenv.2023.119650, 2023.

Mann, H.B.: Non-Parametric Test against Trend. Econometrica, 13, 245-259. http://dx.doi.org/10.2307/1907187, 1945.

Ng, N. L., Herndon, S. C., Trimborn, A., Canagaratna, M. R., Croteau, P. L., Onasch, T. B., Sueper, D., Worsnop, D. R., Zhang, Q., Sun, Y. L., and Jayne, J. T.: An Aerosol Chemical Speciation Monitor (ACSM) for routine monitoring of the composition and mass concentrations of ambient aerosol, Aerosol Sci. Tech., 45, 780–794, 2011.

Niemi, J. v., Saarikoski, S., Aurela, M., Tervahattu, H., Hillamo, R., Westphal, D. L., Aarnio, P., Koskentalo, T., Makkonen, U., Vehkamäki, H., & Kulmala, M.: Long-range transport episodes of fine particles in southern Finland during 1999-2007. Atmos. Environ., 43(6), 1255–1264. https://doi.org/10.1016/j.atmosenv.2008.11.022, 2009.

Ning, Z., & Sioutas, C.: Atmospheric Processes Influencing Aerosols Generated by Combustion and the Inference of Their Impact on Public Exposure: A Review. Aerosol Air Qual. Res., 10(1), 43–58. https://doi.org/10.4209/AAQR.2009.05.0036, 2010.

Oduber, F., Calvo, A. I., Castro, A., Blanco-Alegre, C., Alves, C., Calzolai, G., Nava, S., Lucarelli, F., Nunes, T., Barata, J., & Fraile, R.: Characterization of aerosol sources in León (Spain) using Positive Matrix Factorization and weather types. Sci. Total Environ., 754. https://doi.org/10.1016/j.scitotenv.2020.142045, 2021.

Ogulei, D., Hopke, P. K., & Wallace, L. A.: Analysis of indoor particle size distributions in an occupied townhouse using positive matrix factorization. Indoor Air, 16(3), 204–215. https://doi.org/10.1111/j.1600-0668.2006.00418.x, 2006.

https://doi.org/10.5194/egusphere-2023-2428
Preprint. Discussion started: 8 November 2023

Ogulei, D., Hopke, P. K., Zhou, L., Patrick Pancras, J., Nair, N., & Ondov, J. M.: Source apportionment of Baltimore aerosol from combined size distribution and chemical composition data. Atmos. Environ., 40(SUPPL. 2), 396–410. https://doi.org/10.1016/j.atmosenv.2005.11.075, 2006.

Paatero, P.: Least squares formulation of robust non-negative factor analysis. Chemom. Intell. Lab. Syst., 37(1), 23–35. https://doi.org/10.1016/S0169-7439(96)00044-5, 1997.

Pirjola, L., Niemi, J. V., Saarikoski, S., Aurela, M., Enroth, J., Carbone, S., Saarnio, K., Kuuluvainen, H., Kousa, A., Rönkkö, T., & Hillamo, R.: Physical and chemical characterization of urban winter-time aerosols by mobile measurements in Helsinki, Finland. Atmos. Environ., 158, 60-75. https://doi.org/10.1016/j.atmosenv.2017.03.028, 2017.

Rivas, I., Beddows, D. C. S., Amato, F., Green, D. C., Järvi, L., Hueglin, C., Reche, C., Timonen, H., Fuller, G. W., Niemi, J. V., Pérez, N., Aurela, M., Hopke, P. K., Alastuey, A., Kulmala, M., Harrison, R. M., Querol, X., & Kelly, F. J.: Source apportionment of particle number size distribution in urban background and traffic stations in four European cities. Environ. Int., 135(November 2019), 105345. https://doi.org/10.1016/j.envint.2019.105345. 2020.

Rönkkö, T., Kuuluvainen, H., Karjalainen, P., Keskinen, J., Hillamo, R., Niemi, J. V., Pirjola, L., Timonen, H. J., Saarikoski, S., Saukko, E., Järvinen, A., Silvennoinen, H., Rostedt, A., Olin, M., Yli-Ojanperä, J., Nousiainen, P., Kousa, A., & Dal Maso, M.: Traffic is a major source of atmospheric nanocluster aerosol. Proc. Natl. Acad. Sci. U.S.A., 114(29), 7549–7554. https://doi.org/10.1073/PNAS.1700830114/SUPPL_FILE/PNAS.201700830SI.PDF, 2017.

Rose, C., Collaud Coen, M., Andrews, E., Lin, Y., Bossert, I., Lund Myhre, C., Tuch, T., Wiedensohler, A., Fiebig, M., Aalto, P., Alastuey, A., Alonso-Blanco, E., Andrade, M., Artíñano, B., Arsov, T., Baltensperger, U., Bastian, S., Bath, O., Beukes, J. P., Brem, B. T., Bukowiecki, N., Casquero-Vera, J. A., Conil, S., Eleftheriadis, K., Favez, O., Flentje, H., Gini, M. I., Gómez-Moreno, F. J., Gysel-Beer, M., Hallar, A. G., Kalapov, I., Kalivitis, N., Kasper-Giebl, A., Keywood, M., Kim, J. E., Kim, S.-W., Kristensson, A., Kulmala, M., Lihavainen, H., Lin, N.-H., Lyamani, H., Marinoni, A., Martins Dos Santos, S., Mayol-Bracero, O. L., Meinhardt, F., Merkel, M., Metzger, J.-M., Mihalopoulos, N., Ondracek, J., Pandolfi, M., Pérez, N., Petäjä, T., Petit, J.-E., Picard, D., Pichon, J.-M., Pont, V., Putaud, J.-P., Reisen, F., Sellegri, K., Sharma, S., Schauer, G., Sheridan, P., Sherman, J. P., Schwerin, A., Sohmer, R., Sorribas, M., Sun, J., Tulet, P., Vakkari, V., van Zyl, P. G., Velarde, F., Villani, P., Vratolis, S., Wagner, Z., Wang, S.-H., Weinhold, K., Weller, R., Yela, M., Zdimal, V., and Laj, P.: Seasonality of the particle number concentration and size distribution: a global analysis retrieved from the network of Global Atmosphere Watch (GAW) near-surface observatories, Atmos. Chem. Phys., 21, 17185–17223, https://doi.org/10.5194/acp-21-17185-2021, 2021.

Saarikoski, S., Hellén, H., Praplan, A. P., Schallhart, S., Clusius, P., Niemi, J. V., Kousa, A., Tykkä, T., Kouznetsov, R., Aurela, M., Salo, L., Rönkkö, T., Barreira, L. M. F., Pirjola, L., and Timonen, H.: Characterization of volatile organic compounds and submicron organic aerosol in a traffic environment. Atmos. Chem. Phys., 23(5), 2963–2982. https://doi.org/10.5194/ACP-23-2963-2023, 2023.

Sen, P. K.: Estimates of the regression coefficient based on Kendall's tau. J. Amer. Statist. Assoc., 63, 1379-1389., 1968.

https://doi.org/10.5194/egusphere-2023-2428
Preprint. Discussion started: 8 November 2023

Tauler, R., Viana, M., Querol, X., Alastuey, A., Flight, R. M., Wentzell, P. D., and Hopke, P. K.: Comparison of the results obtained by four receptor modelling methods in aerosol source apportionment studies. Atmos. Environ., 43(26), 3989–3997. https://doi.org/10.1016/j.atmosenv.2009.05.018, 2009.

Teinilä, K., Timonen, H., Aurela, M., Kuula, J., Rönkkö, T., Hellèn, H., Loukkola, K., Kousa, A., Niemi, J. v., and Saarikoski, S.: Characterization of particle sources and comparison of different particle metrics in an urban detached housing area, Finland. Atmos. Environ., 272. https://doi.org/10.1016/j.atmosenv.2022.118939, 2022.

Theil, H.: A rank-invariant method of linear and polynomial regression analysis, I. Proc. Kon. Ned. Akad. v. Wetensch.A53, 386-392. 1950

Timonen, H., Saarikoski, S., Tolonen-Kivimä, O., Aurela, M., Saarnio, K., Petäjä, T., Aalto, P. P., Kulmala, M., Pakkanen, T., & Hillamo, R. Size distributions, sources and source areas of water-soluble organic carbon in urban background air. Atmos. Chem. Phys., 8(18), 5635–5647. https://doi.org/10.5194/ACP-8-5635-2008, 2008.

WHO: WHO global air quality guidelines. Coastal And Estuarine Processes, 1–360., 2021.

Wiedensohler, A., Birmili, W., Nowak, A., Sonntag, A., Weinhold, K., Merkel, M., Wehner, B., Tuch, T., Pfeifer, S., Fiebig, M., Fjäraa, A. M., Asmi, E., Sellegri, K., Depuy, R., Venzac, H., Villani, P., Laj, P., Aalto, P., Ogren, J. A., Swietlicki, E., Williams, P., Roldin, P., Quincey, P., Hüglin, C., Fierz-Schmidhauser, R., Gysel, M., Weingartner, E., Riccobono, F., Santos, S., Grüning, C., Faloon, K., Beddows, D., Harrison, R., Monahan, C., Jennings, S. G., O'Dowd, C. D., Marinoni, A., Horn, H.-G., Keck, L., Jiang, J., Scheckman, J., McMurry, P. H., Deng, Z., Zhao, C. S., Moerman, M., Henzing, B., de Leeuw, G., Löschau, G., and Bastian, S.: Mobility particle size spectrometers: harmonization of technical standards and data structure to facilitate high quality long-term observations of atmospheric particle number size distributions, Atmos. Meas. Tech., 5, 657–685, https://doi.org/10.5194/amt-5-657-2012, 2012.

Wu, J., Zhu, J., Li, W., Xu, D., & Liu, J.: Estimation of the PM2.5 health effects in China during 2000–2011. Environmental Sci. Pollut. Res., 24(11), 10695–10707. https://doi.org/10.1007/s11356-017-8673-6, 2017.

Wu, T., & Boor, B. E. (2021). Urban aerosol size distributions: a global perspective.: Atmos. Chem. Phys., 21(11), 8883–8914. https://doi.org/10.5194/acp-21-8883-2021, 2021.

Zhou, L., Kim, E., Hopke, P. K., Stanier, C., & Pandis, S. N.: Mining airborne particulate size distribution data by positive matrix factorization., J. Geophys. Res. Atmos, 110(7), 1–15. https://doi.org/10.1029/2004JD004707, 2005.